Two-quantum photon-phonon laser

A A Zadernovsky

Moscow State Technical University of Radioengineering, Electronics and Automation, Department of Physics, 78 Vernadsky Ave., 119454 Moscow, RUSSIA

E-mail: zadernovsky@mirea.ru

Abstract. We discuss a new approach to the implementation of laser action in silicon and other indirect band gap semiconductors – two-quantum photon-phonon laser. Dynamics of the photon-phonon laser generation in indirect band gap semiconductors with electron population inversion is investigated in detail with aid of the rate equations. Numerical estimates are made for Si and Ge.

1. Introduction

The possibility to exploit indirect band gap semiconductors as an active medium for lasers is discussed by researchers for many years. Already in the first publication on this subject [1], which appeared shortly after demonstration of the first semiconductor laser, it has been concluded that indirect band gap semiconductors are not suitable for light emitting devices and realizing a laser. In such semiconductors the bottom of the conduction band is not located directly above the top of the valence band in the momentum space of a crystal. This means that an electron in the conduction band can not to have the same momentum as a hole in the valence band. As a result, the near-to-gap radiative electron-hole recombination can only occur through two-quantum transitions with emission of a photon and simultaneous emission or absorption of a phonon to satisfy the laws of energy and momentum conservation. The rate of such two-quantum transitions is very low and therefore, indirect band gap semiconductors are highly inefficient as a host material for light sources.

Despite this disappointing conclusion researchers do not leave the efforts to find a solution to this problem [2–5]. The reason for such persistence is silicon – one of the most famous and attractive indirect band gap semiconductors. Silicon is the fundamental material used in the electronics industry. It is exploited as a substrate for most integrated circuits. Therefore, creation of silicon-based light sources (either light emitting diodes or lasers) would pave the way for closer integration of photonics and electronics.

The advent of nanotechnology opened up entirely new possibilities for researchers. Optical properties of a tiny crystal with the size that are comparable to the electron de Broglie wavelength (for instance, less than 5 nm at room temperature) is fundamentally differ from its bulk counterpart. When the dimensions are so small, quantum effects start to play an important role and can fully alter the properties of the original material.

The quantum confinement effects may offer a solution to the problem of silicon and other indirect band gap semiconductors. According to the Heisenberg uncertainty principle, when a particle is spatially localized, its momentum becomes uncertain. This means that in low-dimensional indirect band gap semiconductors (nanocrystals, thin layered structures, porous materials), the tails of the

wavefunctions of an electron and a hole can now partially overlap, allowing the quasi-direct transitions to occur and thus increasing the probability of radiative recombination.

A number of groups have presented the experimental data on the observation of an enhanced luminescence and even an optical gain in nanostructured silicon, namely, in nanocrystals [6, 7], in silicon on insulator superlattices [8] and in nano-porous silicon [9–11]. Soon afterwards, the efficient silicon-based light emitting diodes [12, 13] have been demonstrated.

Silicon laser is the ultimate goal for researchers and a number of important breakthroughs have been made in the past decade [14]. Among the impressive achievements are the first demonstration of a pulsed silicon Raman laser [15] and the first successful demonstration of a CW silicon Raman laser shortly thereafter [16].

Raman laser is a specific type of laser where the light-amplification mechanism is stimulated Raman scattering. The optical pumping in Raman lasers does not produce a population inversion. The pumping radiation is rather converted into stimulated radiation in nonlinear laser medium. In contrast, most of the conventional lasers rely on stimulated electronic transitions between inversely populated quantum states. Today all the conventional semiconductor lasers exploit the materials with direct band gap structure while the lasers on indirect band gap semiconductors remain still elusive despite the efforts of many researchers [17–22].

In this paper we discuss a new approach to the implementation of laser action in indirect band gap semiconductors – two-quantum photon-phonon laser. Dynamics of the photon-phonon laser generation in a bulk indirect band gap semiconductor with electron population inversion is investigated in detail with aid of the rate equations. Numerical estimates are made for Si and Ge.

2. Principles of photon-phonon laser action

Inverted electronic population, maintained in an indirect band gap semiconductor by a pumping, enables the band-to-band electron transitions with emission of a photon. If such transitions occur between the states close to the energy band edges, the emission of a photon must be assisted by simultaneous emission or absorption of a phonon to conserve the momentum (see figure 1).

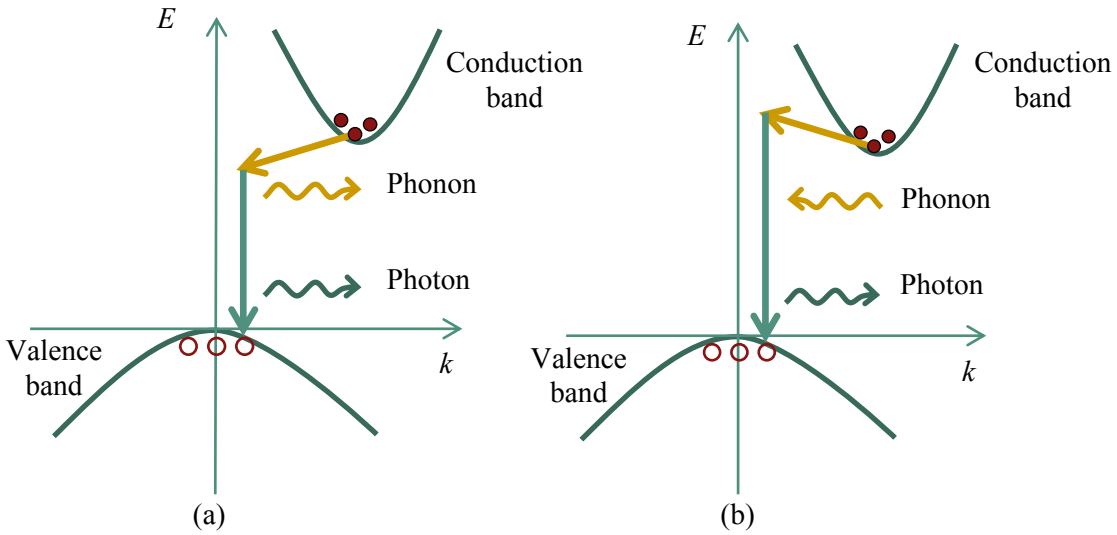

Figure 1. Electron-hole recombination (a) with emission of a phonon and a photon or (b) with absorption of a phonon and emission of a photon.

The rate of such two-quantum transitions and the corresponding photon gain in indirect band gap semiconductors is much less than in semiconductors with direct band gap structure, where the similar

radiative transitions are single-quantum. Moreover, as it was pointed out [1] at the very beginning of the study of this problem, the free carrier photon absorption in indirect band gap semiconductors is increased with pumping more rapidly than the photon gain and, thus, in such semiconductors the photon laser action seems to be impossible.

The photon emission rate, however, could be increased by stimulating the phonon part of the two-quantum transitions with the help of a phonon flux injected through a crystal surface from an external acoustic source. At a high enough intensity of this flux and at a high enough level of inverted electronic population, the photon gain could exceed the photon losses and we might expect the photon laser action.

In typical indirect band gap semiconductors such as the crystals of Si and Ge, the phonons that involved in the two-quantum transitions are in THz-frequency range, in which the effective acoustic sources are not available. As a way of getting around this problem, we propose to generate the required phonons directly inside the crystals.

The phonons generated in the two-quantum transitions with emission of a phonon and a photon (figure 2a) can be absorbed in the two-quantum transitions with absorption of a phonon and emission of a photon (figure 2b). Such transitions are known as the Stokes and anti-Stokes vibronic sidebands. Since the phonon energy is much less than that of the photon, the probabilities of these processes are similar. The phonon emission rate, however, can be increased if the photon part of the two-quantum transition with simultaneous emission of a photon and a phonon is stimulated by the light from an appropriate external laser source. Since the energies of the photons radiated in Stokes and anti-Stokes sidebands differ by twice the phonon energy, the separate stimulation of the two-quantum process with phonon emission only is possible within a certain range of laser light frequencies.

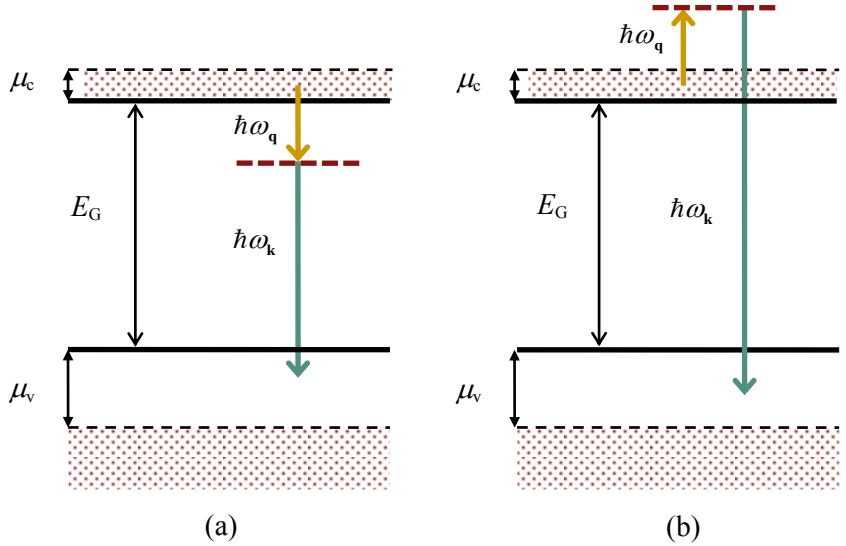

Figure 2. Two-quantum transitions (a) with emission of a phonon and a photon or (b) with absorption of a phonon and emission of a photon.

Moreover, the laser light frequency can be fitted in such a way to promote emission of phonons of only a specific type. Indeed, the luminescence spectrum of indirect electron-hole recombination has the form of a series of peaks corresponding to the different types of phonons involved in the process [23]. If the laser light frequency is close to one of these peaks, the emission rate of the phonons of the specific type is increased. We are interested in transitions involving emission of the transverse acoustic (TA) phonons, since at low temperatures of the crystals (temperature of liquid helium and lower) the phonons of this type are long-lived with respect to anharmonic phonon-phonon interactions (the selection rules forbid the TA phonon decay into two other phonons with lower energies) [24].

At a high enough intensity of the external stimulating radiation and at a high enough level of pumping, the phonon gain can exceed the phonon losses and the phonon laser action appears. The produced phonons can either couple to the anti-Stokes sideband, thus allowing the spectroscopic detection of the beginning of the phonon laser action, or can further stimulate the phonon part of the same transition, leading to a growth of the photon emission rate in the Stokes sideband. This permits us to sustain the phonon laser action by gradual increasing the pumping rate with simultaneous decreasing the intensity of the external stimulating radiation. Finally, the source of stimulating radiation can be switch off and the system continues to operate with simultaneous lasing of both photons and phonons.

3. Photon and phonon emission rates

In this section we consider the emission rates of photons and phonons via the two-quantum photon-phonon transitions in which either the optical or the acoustic components, or both may be stimulated. We follow our article [25], where such transitions have been first examined.

3.1. The rate of stimulated-stimulated photon-phonon transitions

The number of transitions per unit volume per unit time W_{kq} with simultaneous stimulated emission of photons and TA phonons is determined by the expression

$$W_{kq} = R_t N_k N_q \sum_{\mathbf{k}_1 \mathbf{k}_2} \delta_{0,\mathbf{k}_1+\mathbf{q}-\mathbf{k}_2} \delta(E_{c\mathbf{k}_2} - E_{v\mathbf{k}_1} - \hbar\omega_{\mathbf{k}} - \hbar\omega_{\mathbf{q}t})[f_c(E_{\mathbf{k}_2}) - f_v(E_{\mathbf{k}_1})] \quad (1)$$

where N_k is the photon concentration in an optical mode including the photons with energy $\hbar\omega_{\mathbf{k}}$ and wave vectors $\mathbf{k}$ of opposite sign, N_q is the phonon concentration in an acoustic mode representing the total concentration of the TA phonons with energy $\hbar\omega_{\mathbf{q}t}$ and wave vectors $\mathbf{q}$ taking into account all the equivalent phonon propagating directions in a crystal. For example, in silicon there are 6 of such directions along the axes (100), while in germanium there are 8 equivalent directions along the axes (111).

The summation over the wave vectors $\mathbf{k}_1$ and $\mathbf{k}_2$ of electrons in the valence band v and the conduction band c, respectively, runs over the first Brillouin zone and includes the summation over the two electron spin states. The electron energies near the band extrema are

$$\begin{aligned} E_{c\mathbf{k}_2} &= E_G + \hbar^2(\mathbf{k}_2 - \mathbf{q}_0)^2/2m_c\,; \\ E_{v\mathbf{k}_1} &= -\hbar^2\mathbf{k}_1^2/2m_v \end{aligned} \quad (2)$$

where E_G is the energy gap width, m_c, m_v are the electron and the hole effective masses, $\mathbf{q}_0$ is the wave vector of the conduction band minimum pointing from the origin to one of equivalent valleys in the first Brillouin zone. The functions $f_c(E)$, $f_v(E)$ are the quasi-Fermi functions, which are defined at a temperature T by the familiar expression

$$f_{c,v}(E) = \frac{1}{\exp[(E - F_{c,v})/\kappa T] + 1} \quad (3)$$

where $F_c = \mu_c + E_G$, and $F_v = -\mu_v$ represent the quasi-Fermi energy levels in the bands.

The coefficient R_t contains the matrix element of the considered transition. Since the phonon energy is much less than that of the photon this matrix element can be replaced by another one corresponding to the two-quantum transition with photon absorption and TA phonon emission (the only difference between the matrix elements is the sign of the phonon energy). This permits us to determine R_t from data on measurement of the optical absorption coefficient in the region of the absorption edge spectrum of indirect band gap semiconductors. To a good degree of approximation R_t can be regarded as a constant in the vicinity of the band extrema. Taking into account that the transverse acoustic modes are degenerate and using the curves [26] for the optical absorption

coefficient versus photon energy in Si and Ge at temperature T=4.2 K , we obtain [25] $R_t = 4\times10^{-31}$ eV cm^6 c^{-1} for Si and $R_t = 5\times10^{-30}$ eV cm^6 c^{-1} for Ge.

Due to the δ-function and the Kronecker symbol $\delta_{0,\mathbf{k}_1+\mathbf{q}-\mathbf{k}_2}$ the sum (1) is essentially reduced to a sum over all allowed vectors $\mathbf{k}_1$ and $\mathbf{k}_2$, consistent with the conservation of energy and momentum (the momentum of a photon can be neglected). For electron transitions between states close to the band edges, the wave vector $\mathbf{q}$ of the emitted phonons is near to $\mathbf{q}_0$. Therefore, summing in (1) over $\mathbf{k}_2$ at $\mathbf{q}=\mathbf{q}_0$ and then integrating over $\mathbf{k}_1$ (using the density of the electron states), we obtain in the range $\Delta_{\mathbf{q}_0} = \hbar\omega_{\mathbf{k}} + \hbar\omega_{\mathbf{q}_0 t} - E_G > 0$ the following expression

$$W_{kq} = AN_k N_q \left[\left(\exp\frac{\mu_0 - \mu_c}{\kappa T} + 1 \right)^{-1} - \left(\exp\frac{\mu_v - \mu_0\, m_c/m_v}{\kappa T} + 1 \right)^{-1} \right] \tag{4}$$

with

$$A = \frac{R_t}{2\pi^2} \left(\frac{2m_r}{\hbar^2} \right)^{3/2} \Delta_{\mathbf{q}_0}^{1/2} \tag{5}$$

and $m_r = m_c\, m_v/(m_c+m_v)$, $\mu_0 = \Delta_{\mathbf{q}_0}\, m_r/m_c$.

One can see from (4) that in the range $0 < \Delta_{\mathbf{q}_0} < \mu_c + \mu_v$ there is a gain of phonons and photons. At low temperatures, $kT << \mu_0$, the gain maximum is reached at $\mu_c \approx \mu_0$ (taking into account the inequality $\mu_v > \mu_c\, m_c/m_v$ that follows from the condition of electric neutrality of a semiconductor). In this case we can neglect the second term in (4).

Once a level of μ_c , which is maintained by a pumping, is fixed, the optimum photon energy of externally applied stimulating radiation is determined from the condition $\mu_0 = \mu_c$. The pumping, in turn, is limited by the requirement of emission of TA phonons only. If the stimulating radiation promotes emission of phonons of several types, the quantum efficiency of the TA phonon generating process, which we are interested in, is decreased. Combined application of these requirements determines the optimum pumping condition $\mu_c^{opt} = 1.5\times10^{-2}$ eV for Si and $\mu_c^{opt} = 0.8\times10^{-2}$ eV for Ge and the optimum photon energy of stimulating radiation $\hbar\omega_{\mathbf{k}_0}$ =1.165 eV for Si and $\hbar\omega_{\mathbf{k}_0}$ = 0.745 eV for Ge. Using the data for Si and Ge [26] collected in table 1, we obtain for the rate constant A (5) at the optimum photon energy the following value $A = 0.4\times10^{-10}$ cm^3 s^{-1} for Si and $A = 1.9\times10^{-10}$ cm^3 s^{-1} for Ge.

Table 1.

Semi-conductor	Type of phonon	Phonon energy, eV	Effective mass		Energy gap width (T=0), eV	q_0, 10^{-8} cm^{-1}
			m_c/m_0	m_v/m_0		
Si	*Acoustic:*		0.33	0.61	1.16	0.94
	transverse (TA)	0.018				
	longitudinal (LA)	0.027				
	Optical:					
	longitudinal (LO)	0.091				
	transverse (TO)	0.122				
Ge	*Acoustic:*		0.22	0.35	0.74	0.96
	transverse (TA)	0.008				
	longitudinal (LA)	0.027				

3.2. The rate of stimulated-spontaneous photon-phonon transitions

The rate of stimulated-spontaneous transitions W_{k0} with stimulated photon emission into an optical mode and spontaneous phonon emission is determined by the expression

$$W_{k0} = R_t N_k N_c \sum_{\mathbf{q}} \sum_{\mathbf{k}_1 \mathbf{k}_2} \delta_{0,\mathbf{k}_1+\mathbf{q}-\mathbf{k}_2} \delta(E_{c\mathbf{k}_2} - E_{v\mathbf{k}_1} - \hbar\omega_{\mathbf{k}} - \hbar\omega_{\mathbf{q}t}) f_c(E_{\mathbf{k}_2})[1 - f_v(E_{\mathbf{k}_1})] \quad (6)$$

where N_c is the number of the equivalent conduction band valleys ($N_c = 6$ for Si and $N_c = 4$ for Ge). The summation over **q** runs over the wave vectors of TA phonons only, since in the range of the optimum pumping it is the only type of the phonons participating in the process.

At low temperatures the quasi-Fermi functions in (6) can be well approximated by the step function $f_{c,v}(E) = \Theta(F_{c,v} - E)$. Summing over **q**, taking into account the two TA phonon polarizations, and then integrating over $\mathbf{k}_1$ and $\mathbf{k}_2$, we obtain

$$W_{k0} = CN_k f(\mu_c/\mu_0) \quad (7)$$

with

$$C = R_t \frac{N_c}{4\pi^3} \left(\frac{m_c}{\hbar^2}\right)^{3/2} \left(\frac{m_v}{\hbar^2}\right)^{3/2} \Delta_{\mathbf{q}_0}^2 . \quad (8)$$

The function $f(\mu_c/\mu_0)$ in (7) is equal to 0 at $\mu_c/\mu_0 \le (1+m_c/m_v)/(1+ N_c^{2/3} m_c/m_v)$, is equal to 1 at $\mu_c/\mu_0 \ge 1+m_c/m_v$ and of the order of 1 at other cases. In particular, at the gain maximum, when $\mu_0 = \mu_c$, we have $f(1) \approx 0.7$ both for Si and Ge . At the optimum photon energy of stimulating radiation we obtain for the rate constant C (8) the following estimates $C = 2.1\times10^9$ s^{-1} for Si and $C = 1.3\times10^9$ s^{-1} for Ge.

3.3. The rate of spontaneous-stimulated photon-phonon transitions

The rate of spontaneous-stimulated transitions W_{0q} with spontaneous photon emission and stimulated TA phonon emission into an acoustic mode is determined by the expression

$$W_{0q} = R_t N_q \sum_{\mathbf{k}} \sum_{\mathbf{k}_1 \mathbf{k}_2} \delta_{0,\mathbf{k}_1+\mathbf{q}-\mathbf{k}_2} \delta(E_{c\mathbf{k}_2} - E_{v\mathbf{k}_1} - \hbar\omega_{\mathbf{k}} - \hbar\omega_{\mathbf{q}t}) f_c(E_{\mathbf{k}_2})[1 - f_v(E_{\mathbf{k}_1})] \quad (9)$$

where the summation over the photon wave vectors **k** includes the summation over the two photon polarizations. Summing in (9) over $\mathbf{k}_2$ at $\mathbf{q}=\mathbf{q}_0$ and then performing the integration over $\mathbf{k}_1$ and **k**, taking into account that $\hbar\omega_{\mathbf{q}_0 t} << E_G$, we obtain

$$W_{0q} = DN_q N_e \quad (10)$$

where

$$D = \frac{R_t}{N_c} \frac{E_G^2}{\pi^2 (\hbar c)^3} \quad (11)$$

c is the velocity of light in the material ($c = 0.88\times 10^{10}$cm s^{-1} for Si and $c = 0.75\times 10^{10}$cm s^{-1} for Ge) and N_e is the electron concentration in the conduction band which is connected with μ_c by the relation

$$N_e = \frac{N_c}{3\pi^2} \left(\frac{2m_c}{\hbar^2}\right)^{3/2} \mu_c^{3/2} \quad (12)$$

The estimates for the rate constant D (11) give D=0.5×10^{16} cm^3 s^{-1} for Si and D=5.7×10^{16} cm^3 s^{-1} for Ge. The electron concentration (12) is estimated at the condition of $\mu_c = \mu_0$ by the value of N_e = 8.9×10^{18} cm^{-3} for Si and N_e = 1.3×10^{18} cm^{-3} for Ge.

3.4. The rate of spontaneous-spontaneous photon-phonon transitions

The rate of spontaneous-spontaneous photon-phonon transitions W_{00} can be expressed as follows [27]

$$W_{00} = BN_e^2 \tag{13}$$

with the rate constant B=0.2×10^{-14} cm^3 s^{-1} for Si and B=3.4×10^{-14} cm^3 s^{-1} for Ge.

4. Photon and phonon losses

4.1. Phonon losses

The TA phonons emitted into a particular acoustic mode can leave the mode (a) due to the phonon absorption in the two-quantum transitions with simultaneous photon radiation in the anti-Stokes sideband (see figure 2b), (b) due to anharmonic interaction with heat phonons (lattice absorption), (c) due to the phonon scattering by free carriers and (d) by the lattice imperfections (impurities, vacancies, dislocations).

(a) Since $\hbar\omega_{\mathbf{q}t} << \hbar\omega_{\mathbf{k}}$, the rate of the phonon coupling to the anti-Stokes sideband is similar to the rate of spontaneous-stimulated transitions W_{0q} (9). Therefore, the inverse lifetime τ_A^{-1} of the TA phonon with wave vector $\mathbf{q}_0$ can be estimated by the expression $\tau_A^{-1} = DN_e$, where N_e is the electron concentration (12). At the condition of the gain maximum $\mu_c=\mu_0$, we obtain τ_A^{-1}=4.5×10^2 s^{-1} for Si and τ_A^{-1} = 7.4× 10^2 s^{-1} for Ge.

(b) The inverse lifetime τ_t^{-1} of the TA phonon with wave vector $\mathbf{q}_0$ in phonon-phonon interactions can be estimated [24] by the value of τ_t^{-1} = 10^3÷10^4 s^{-1} for Si and τ_t^{-1} = 10^2÷10^3 s^{-1} for Ge at a temperature of the crystals of T= 1 K.

(c) Phonon absorption by free carriers obeys certain selection rules. It vanishes for TA phonons with wave vector $\mathbf{q}$ along any symmetry axis of the spheroidal Fermi surface [28]. In our case, the absorption of TA phonons with wave vector $\mathbf{q}_0$ is essentially forbidden by the selection rules. Thus for $\mathbf{q}$ near $\mathbf{q}_0$, the TA phonon absorption by free carriers can be neglected.

(d) Among all the above listed channels of TA phonon losses, elastic Rayleigh scattering by isotope impurities is the largest one in an otherwise perfect crystal [29]. For Si and Ge with natural isotopic abundances the inverse lifetime τ_i^{-1} of the TA phonon with wave vector $\mathbf{q}_0$ is estimated by [30] τ_i^{-1} =7.2×10^9 s^{-1} for Si and τ_i^{-1}= 5.2×10^8 s^{-1} for Ge. We will assume that the last two values can be reduced with the help of isotope separation methods by 3–4 orders of magnitude.

Summarizing all the above estimates we may conclude that the crucial contribution to the phonon losses from a particular acoustic mode gives the phonon scattering by isotope impurities. Thus, in sufficiently pure (including isotopic purity) and perfect crystals of Si and Ge, the total inverse lifetime of the TA phonon in an acoustic mode can be estimated by the value of τ_0^{-1} =7×10^5 s^{-1} for Si and τ_0^{-1} = 5×10^4 s^{-1} for Ge .

4.2. Photon losses

Photon losses from a particular optical mode are due to (a) the photon absorption by free carriers, (b) the photon scattering by optical inhomogeneities, (c) due to diffraction losses and (d) the losses of radiation through the partially reflecting crystal surfaces. We assume that the crystals under investigation are perfect enough to neglect the photon scattering by the optical inhomogeneities. As far as diffraction losses are concerned, one can expect that similar to the semiconductor lasers such losses can be generally reduced by waveguiding of the gain region. Thus, the bulk photon losses are dominated by the free carrier absorption with the rate

$$W_e = \sigma c N_k N_e, \tag{14}$$

where σ is the photon capture cross section ($\sigma = 6\times10^{-18}$ cm^2 for Si and $\sigma = 4\times10^{-18}$ cm^2 for Ge). The rate of photon losses due to radiation through the end crystal surfaces of reflectivity R ($R = 0.30$ for Si and $R = 0.36$ for Ge) is equal to N_k/τ, where

$$\tau^{-1} = \frac{c}{L}\ln(1/R) \tag{15}$$

and L is the crystal length. Assuming $L = 250\ \mu$m, we obtain $\tau^{-1} = 3.5\times10^{11}$ s^{-1} for Si and $\tau^{-1} = 3\times10^{11}$ s^{-1} for Ge.

5. Rate equations

The dynamics of the photon-phonon generation in indirect band gap semiconductors can be described by the following set of the rate equations for the electron concentration N_e in the conduction band, the photon concentration N_k in an optical mode, and for the phonon concentration N_q in an acoustic mode

$$\frac{dN_e}{dt} = W_p - W_{kq} - W_{k0} - W_{0q} - W_{00} \tag{16}$$

$$\frac{dN_k}{dt} = \frac{1}{\tau}\left(\frac{1+R}{1-R}nN_0 - N_k\right) + W_{kq} + W_{k0} - W_e \tag{17}$$

$$\frac{dN_q}{dt} = W_{kq} - \frac{N_q}{\tau_0} \tag{18}$$

where W_p is the pumping rate of electrons into the conduction band, N_0 is the photon concentration of stimulating radiation outside the crystal, the term $nN_0(1+R)/(1-R)$, where n is the refractive index, represents the stationary photon concentration which is sustained in an optical mode inside the crystal with aid of the external simulating radiation.

In the equation (17) we neglect the spontaneous photon contribution into the optical mode, as well as in (18) we neglect the contribution of spontaneous phonons into the acoustic mode. This can be done due to the strict localization of the photons and the phonons in the modes. The contribution into the acoustic mode due to spontaneous-stimulated transitions W_{0q} (10) is balanced by the absorption of the phonons through coupling to the anti-Stokes sideband (see figure 2b). As a result, these terms cancel each other in the equation (18). Furthermore, the term W_{0q} could be omitted in equation (16), since for the steady state solutions, which we are interested in, we have $W_{kq} >> W_{0q}$.

To simplify the rate equations a conversion of variables to dimensionless units is made: $n_e = N_e/N$, $n_k = N_k/N$, $n_q = N_q/(N\tau_0/\tau)$, $\theta = t/\tau$, where the normalizing particle concentration N is determined by the condition $AN\tau_0 = 1$. Using the normalized variables, the rate equations (16–18) can be rewritten as follows

$$\frac{dn_e}{d\theta} = \frac{W_p}{W_0} - n_k n_q S - C\tau m_k f(\mu_c/\mu_0) - B\tau N n_e^2 \tag{19}$$

$$\frac{dn_k}{d\theta} = \frac{1+R}{1-R}nn_0 - n_k + n_k n_q S + C\tau m_k f(\mu_c/\mu_0) - \sigma c\tau N n_k n_e \tag{20}$$

$$\frac{dn_q}{d\theta} = \frac{\tau}{\tau_0}(n_k n_q S - n_q) \tag{21}$$

where $n_0 = N_0/N$; $W_0 = N/\tau$ and $S = \{\exp[(\mu_0 - \mu_c)/kT]+1\}^{-1}$. Equations (19–21) with the relation (12) rewritten through the normalized variables as

$$n_e = \frac{N_c}{3\pi^2 N}\left(\frac{2m_c}{\hbar^2}\right)^{3/2}\mu_c^{3/2} \tag{22}$$

represent the complete set of equations for describing the dynamics of the photon-phonon generation in indirect band gap semiconductors.

6. Dynamics of photon-phonon laser action

We restrict ourselves to the steady state solutions of the rate equations. As it is seen from (21) at $dn_q/d\theta = 0$, there are two types of these solutions: below the phonon lasing threshold with $n_q = 0$ and above the phonon lasing threshold with $n_q \neq 0$. These solutions are shown in the figure 3 (curves of type I and type II, respectively) in the form of dependence of the normalized photon concentration n_k in an optical mode versus the normalized pumping rate W_p/W_0 with the normalized photon concentration n_0 of external stimulating radiation taken as a parameter of a family of curves. Numerical values in the figure 3 correspond to the silicon crystal.

It can be shown [31] with the help of Routh-Hurwitz criterion that only increasing parts of the curves II in figure 3 correspond to the stable steady state solutions. The intersection in the point A between the stable branch of a curve II and a curve I with the same n_0 determines the phonon lasing pumping threshold $(W_p/W_0)_{th}$ and the threshold value for the normalized photon concentration $(n_k)_{th}$ inside the crystal. If the pumping is further increased the system goes on the stable branch of the curve II and the phonon laser action occurs. This leads to a growth of the phonon and the photon concentrations in the modes. If the pumping rate W_p/W_0 exceeds some threshold value W_s/W_0 , the external source of stimulating radiation can be switched off and the system goes from the point C_1 to the working point C_2 on the stable branch of the curve II with $n_0 = 0$. Thus, the system continues to operate with simultaneous lasing of both photons and phonons.

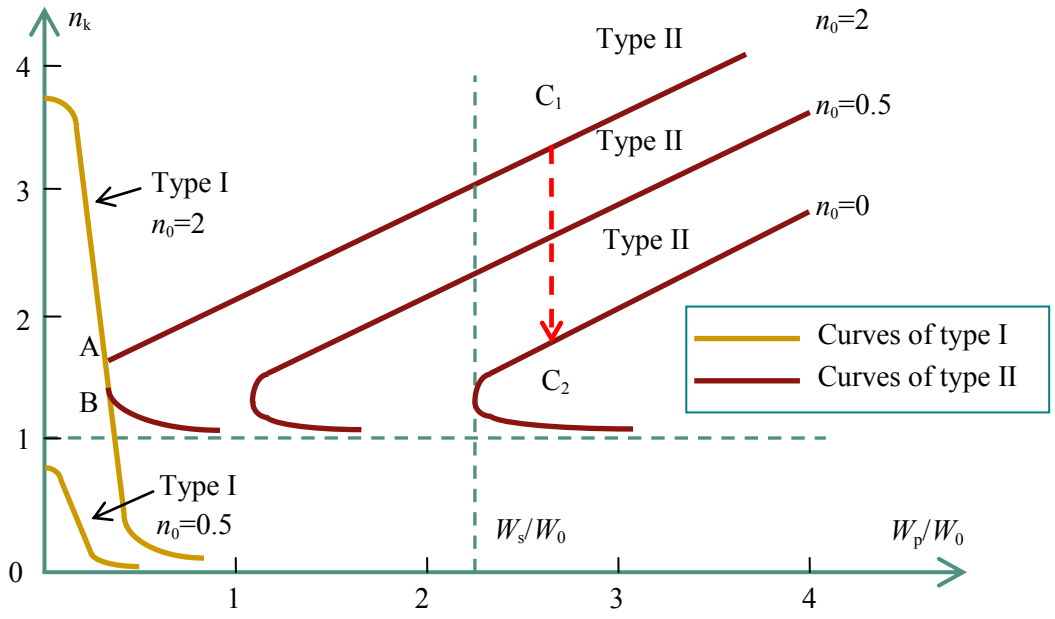

Figure 3. The steady state solutions of the rate equations for Si.

Numerical estimates [31, 32] are collected in the table 2.

Table 2. Numerical estimates

Semicon-ductor	N, 10^{14} cm^{-3}	W_0, 10^{25} cm^{-3}c^{-1}	$(W_p/W_0)_{th}$, 10^{-3}	$(n_k)_{th}$	W_s/W_0	n_{ks}	n_{qs}	n_0
Si	1.6×10^2	5.6×10^2	4.2	1.6	2.4	3.0	2.4	2.0
Ge	2.6	7.8	3.7	1.8	1.1	3.2	1.1	1.0

N	the normalizing particle concentration
W_0	the normalizing pumping rate
$(W_p/W_0)_{th}$	the normalized threshold pumping rate for starting the phonon laser action
$(n_k)_{th}$	the normalized threshold photon concentration inside the crystal for starting the phonon laser action
W_s/W_0	the normalized threshold pumping rate for starting the simultaneous laser action of both photons and phonons
n_{ks}	the normalized photon concentration inside the crystal for starting the simultaneous laser action of both photons and phonons
n_{qs}	the normalized phonon concentration for starting the simultaneous laser action of both photons and phonons
n_0	the normalized photon concentration of external stimulating radiation

Returning from normalized to the physical variables, we obtain at the optimum photon energy of stimulating radiation ($\hbar\omega_{\mathbf{k}_0}$ =1.165 eV for Si and $\hbar\omega_{\mathbf{k}_0}$ = 0.745 eV for Ge) the following estimate for the threshold light intensity at the point A in figure 3 $I = c\hbar\omega_{\mathbf{k}_0} N(n_k)_{th}$ =4.2×10^7 W/cm^2 for Si and I = 4.0×10^5 W/cm^2 for Ge and the estimate for the intensity of external stimulating radiation $I = c\hbar\omega_{\mathbf{k}_0} Nn_0$ = 5.2×10^7 W/cm^2 for Si and I = 2.2×10^5 W/cm^2 for Ge. For silicon these values are close to the radiative damage threshold of the semiconductor crystals which consist of $10^7 \div 10^8$ W/cm^2 [27].

7. Conclusions

We propose the use of photon-phonon interband electron transitions in indirect band gap semiconductors to obtain phonon lasing and simultaneous lasing of both photons and phonons.

To drive the process of photon-phonon laser generation, we start with stimulating the photon part of the two-quantum transitions with simultaneous emission of phonons and photons by the light from an appropriate laser source. This leads to a growth of the rate of phonon emission. At a high enough intensity of the external stimulating radiation and at a high enough level of pumping, the phonon gain turns out to be equal to the phonon losses in a particular acoustic mode and the phonon laser action appears. It is then possible to sustain the phonon laser action by gradual increasing the pumping rate with simultaneous decreasing the intensity of the external stimulating radiation. Finally, the source of stimulating radiation can be switch off and the system continues to operate with simultaneous lasing of both photons and phonons.

Dynamics of the photon-phonon laser generation has been investigated in detail with aid of the rate equations. Numerical estimates of the threshold intensity of stimulating radiation, the threshold rate of pumping for starting the phonon lasing and the threshold rate of pumping for starting the simultaneous lasing of both photons and phonons have been made for pure (including isotopic purity) and perfect crystals of Si and Ge.

The threshold intensity of stimulating radiation for Si is close to the radiative damage threshold of the semiconductor crystal. It should be noted, however, that the result of our calculations is strongly dependent on the concentration of isotope impurities in Si. We have assumed above that this

concentration can be reduced with the help of isotope separation methods by four orders of magnitude as compared with the natural isotopic concentration. Otherwise, the threshold intensity of stimulating radiation must be increased in an appropriate number of times. On the contrary, in an isotopically pure silicon crystal, where the phonon losses from an acoustic mode is mainly due to lattice absorption and due to phonon absorption in the anti-Stokes vibronic sideband (see figure 2b), the intensity of stimulating radiation may be reduced by an order of magnitude.

Finally, a few remarks on a parasitic nonradiative recombination, which remains even in the pure and perfect semiconductor crystals. We are talking about well-known Auger recombination which has not been taken into account in the rate equation (16). This is a three-particle process where an excited electron recombines with a hole and the excess energy is transferred to another free carrier rather than emitted in the form of a photon. The rate of Auger recombination is proportional to the third degree of concentration of excited carriers, that is $W_{\text{Auger}} = C_{\text{n}} N_{\text{e}}^3$ with $C_{\text{n}} \sim 10^{-31}\text{cm}^6\text{c}^{-1}$ [33] for undoped Si at room temperature. Taken into account the electron concentration (12) at the gain maximum, $N_{\text{e}} = 8.9\times10^{18}$ cm^{-3} for Si, we obtain for the rate of Auger recombination the value of $W_{\text{Auger}} \sim 10^{26}$ cm^{-3}c^{-1} which is an order of magnitude greater than the rate of pumping required for the photon-phonon lasing (see table 2). These estimates show that Auger recombination may be the dominant mechanism at a high level of pumping in Si.

It should be noted, however, that the above estimate has been made at room temperature of the crystal. Temperature dependence of Auger recombination in silicon has been studied in a range from 243 to 473K [34]. To our knowledge, however, there is no data published on Auger recombination at temperatures of liquid helium and lower. Although the general trend is obvious – the Auger coefficient C_{n} should decrease with temperature.

Moreover, there is evidence [35] that some silicon solar cells are characterized by extremely long carrier recombination lifetimes of the order of some milliseconds. That is, for these solar cells, the nonradiative recombination lifetime is of the order of the radiative lifetime, hence their internal quantum efficiency of light emission is of the order of unity. These results are very encouraging for the use of silicon as an active medium for lasers. In any case, this issue requires further investigation.

Acknowledgements
This research was supported by the Ministry of Education and Science of the Russian Federation.

References

[1] Dumke W P 1962 lnterband transitions and maser action *Phys. Rev.* **127** 1559–63
[2] Ossicini S, Pavesi L, Priolo F Light 2003 *Emitting Silicon for Microphotonics* (Berlin: Springer)
[3] Pavesi L and Lockwood D J 2004 *Silicon Photonics* (Berlin: Springer)
[4] Reed G T and Knights A P 2004 *Silicon Photonics: An Introduction* (Chichester UK: John Wiley)
[5] Reed G T and Knights A P 2008 *Silicon Photonics: The State of the Art* (Chichester UK: John Wiley)
[6] Pavesi L, Dal Negro L, Mazzoleni G, Franzo G and Priolo F 2000 Optical gain in silicon nano-crystals *Nature* **408** 440–4
[7] Pelant I 2011 Optical gain in silicon nanocrystals: current status and perspectives *Phys. Status Solidi* A **208** 625–30.
[8] Lu Z H, Lockwood D J and Baribeau J M 1995 Quantum confinement and light emission in SiO_2/Si superlattices *Nature* **378** 258–60
[9] Cullis A G and Canham L T 1991 Visible light emission due to quantum size effects in highly porous crystalline silicon *Nature* **353** 335–38
[10] Gösele U and Lehmann V 1995 Light-emitting porous silicon *Mater. Chem. Phys.* **40** 253–59
[11] Hirschman K D, Tsybeskov L, Duttagupta S P and Fauchet P M 1996 Silicon-based visible light–emitting devices integrated into microelectronic circuits *Nature* **384** 338–41
[12] Wai Lek Ng, Lourenço M A, Gwilliam R M, Ledain S, Shao G and Homewood K P 2001 An

efficient room-temperature silicon-based light-emitting diode *Nature* **410** 192–4
[13] Homewood K P and Lourenço M A 2005 Light from Si via dislocation loops *Matrials Today* **8** No 1 34–9.
[14] Di Liang and Bowers J E 2010 Recent progress in lasers on silicon *Nature Photonics* **4** 511–7
[15] Boyraz O and Jalali B 2004 Demonstration of a silicon Raman laser *Optics Express* **12** 5269–73
[16] Rong H, Jones R, Liu A, Cohen O, Hak D, Fang A and Paniccia M 2005 A continuous-wave Raman silicon laser *Nature* **433** 725–7
[17] Iyer S S and Xie Y H 1993 Light emission from silicon *Science* **260** 40–6
[18] Kimerling L C, Kolenbrander K D, Michel J, and Palm J 1997 Light emission from silicon *Solid State Physics* **50** 333.
[19] Trupke T, Green M A and Würfel P 2003 Optical gain in materials with indirect transitions *J. Appl. Phys.* **93** 9058–61
[20] Chen M J, Tsai C S and Wu M K 2006 Optical gain and co-stimulated emissions of photons and phonons in indirect bandgap semiconductors *Jpn. J. Appl. Phys.* **45** No 8B 6576–88
[21] Pavesi L 2008 Silicon-based light sources for silicon integrated circuits *Advances in Optical Technologies* **2008** 416926.
[22] Pavesi L 2005 Routes towards a silicon-based laser *Materials Today* **8** 18–25
[23] Haynes J R, Lax M and Flood W F 1959 *J. Phys. Chem. Solids* **8** 392
[24] Orbach R 1966 *Phys. Rev. Lett.* **16** 15
[25] Zadernovsky A A and Rivlin L A 1991 Stimulated two-quantum photon-phonon transitions in indirect-gap semiconductors *Sov. J. Quantum Electron*. **21** 255–260
[26] McLean T P 1960 The absorption edge spectrum of semiconductors *Progress in semiconductors* Vol. 5 (London: Heywood) p 53
[27] Pankove J I 1971 *Optical processes in semiconductors* (New Jersey: Englewood Cliffs) chapters 3–6
[28] Hensel J C and Dynes R C 1980 *Phonon scattering in condensed matter* ed Maris H J (New York: Plenum Press) p 395
[29] Bron W E 1985 *Nonequilibrium phonon dynamics (NATO ASI series:* ser B, vol 124*)* ed Bron W E (New York: Plenum Press) p 5
[30] Holland M C 1963 *Phys. Rev.* **132** 2461
[31] Zadernovsky A A and Rivlin L A 1993 Photon-phonon laser action in indirect-gap semiconductors *Quantum Electron.* **23** 300–308
[32] Zadernovsky A A and Rivlin L A 1993 Photon-phonon lasing in indirect gap semiconductors *Optics Communications* **100** 322–330
[33] Svantesson K G and Nilsson N G 1979 The temperature dependence of the Auger recombination coefficient of undoped silicon *J. Phys.* C: *Solid State Phys.* **12** 5111
[34] Wang S and Macdonald D 2012 Temperature dependence of Auger recombination in highly injected crystalline silicon *J. Appl. Phys.* **112** 113708
[35] Green M A, Zhao J, Wang A, Reece P J and Gal M 2001 Efficient silicon light-emitting diodes *Nature* **412** 805–808